

Silver Nanoparticle–Oligonucleotide Conjugates Based on DNA with Triple Cyclic Disulfide Moieties

Jae-Seung Lee, Abigail K. R. Lytton-Jean, Sarah J. Hurst, and Chad A. Mirkin*

*Department of Chemistry and International Institute for Nanotechnology,
Northwestern University, 2145 Sheridan Road, Evanston, Illinois 60208*

Received May 11, 2007; Revised Manuscript Received May 30, 2007

ABSTRACT

We report a new strategy for preparing silver nanoparticle–oligonucleotide conjugates that are based upon DNA with cyclic disulfide-anchoring groups. These particles are extremely stable and can withstand NaCl concentrations up to 1.0 M. When silver nanoparticles functionalized with complementary sequences are combined, they assemble to form DNA-linked nanoparticle networks. This assembly process is reversible with heating and is associated with a red shifting of the particle surface plasmon resonance and a concomitant color change from yellow to pale red. Analogous to the oligonucleotide-functionalized gold nanoparticles, these particles also exhibit highly cooperative binding properties with extremely sharp melting transitions. This work is an important step toward using silver nanoparticle–oligonucleotide conjugates for a variety of purposes, including molecular diagnostic labels, synthons in programmable materials synthesis approaches, and functional components for nanoelectronic and plasmonic devices.

The discovery and development of DNA-functionalized gold nanoparticle conjugates (DNA–Au NPs) in 1996^{1,2} has opened up opportunities for fundamental studies of their novel properties^{3–6} as well as their application in the assembly of advanced superstructures,^{1,2,7} the detection of nucleic acids, proteins, metal ions, and small molecules^{8–22} and as gene silencing agents.²³ The utility of DNA–Au NPs is, in part, due to their intense optical, catalytic, and synthetically programmable recognition properties. In addition, when chemically modified in the appropriate manner, they can exhibit highly cooperative binding properties, which are typically characterized by extremely sharp melting transitions.⁴ The identification of this cooperativity has led to the development of molecular diagnostic probes that exhibit much higher selectivity and sensitivity for target analytes than conventional molecular fluorophore probes,^{8,19,24–26} and “antisense particle” agents that are significantly more effective at gene knockdown than free DNA-based antisense agents.²³

Silver nanoparticles (Ag NPs) also have generated significant scientific and technological interest.^{27–29} These particles exhibit higher extinction coefficients relative to gold nanoparticles of the same size, possess a particle size-dependent surface plasmon resonance between ~390 and 420 nm, are electrochemically and catalytically active, and exhibit Raman enhancement properties.^{28–31} As has been extensively

demonstrated with gold,^{1,4,32,33} a common method used to functionalize the surface of noble metals is the adsorption of thiol-containing molecules. However, there have been only a few reports of thiol-functionalized Ag NPs,^{34,35} and of the structures prepared, they all (1) show limited stability in saline buffer (up to 0.3 M salt concentration), (2) typically require lengthy synthetic procedures (more than 2 days), and (3) do not exhibit highly cooperative binding as determined by melting analyses (the melting transitions for the hybridized particle aggregates span ≥ 10 °C). Moreover, the possible oligonucleotides that can be used to stabilize the particles are limited with respect to sequence (e.g., poly adenine (A) sequences).^{34,35} These limitations are primarily due to the chemical degradation of the Ag NPs under the functionalization conditions and the susceptibility of the silver surface to oxidation.^{27,36}

As a result of these limitations, alternative approaches have been developed to enable the conjugation of DNA to Ag NPs. Attempts to modify the Ag NP surface with more tailorable and robust materials such as gold, silica, or polymers have been considered.^{27,37–39} However, they require additional cumbersome chemical modification steps. Herein, we present a method to functionalize Ag NPs with oligonucleotides modified with terminal cyclic disulfide groups. These DNA-functionalized silver particles (DNA–Ag NPs) can be synthesized in less than 30 min and show stability at high salt concentrations (1.0 M NaCl). Significantly, the DNA–Ag NPs also exhibit high cooperativity as character-

* To whom correspondence should be addressed. E-mail: chadnano@northwestern.edu.

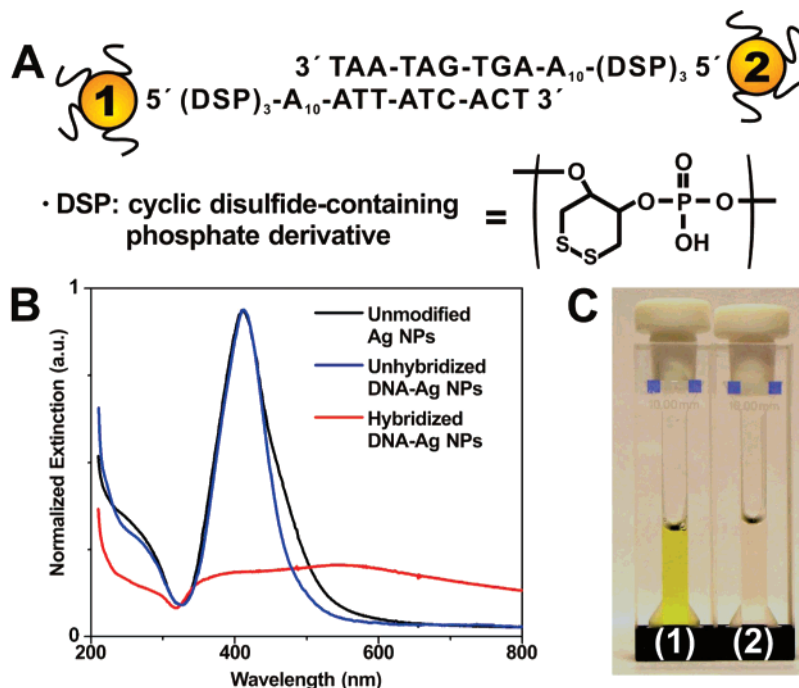


Figure 1. (A) Schematic illustration of the hybridization of two complementary DNA-Ag NPs. (B) UV-vis spectra of unmodified Ag NPs (black line), unhybridized DNA-Ag NPs (blue line), and hybridized DNA-Ag NPs (red line). Note that the wavelength at which the maximum of the extinction of Ag NPs is obtained remains the same after DNA functionalization. After hybridization, however, the band of DNA-Ag NPs broadens and red shifts significantly from 410 to 560 nm. (C) Colorimetric change responsible for the assembly process of DNA-Ag NPs. The intense yellow color of the unhybridized Ag NPs (C1) turns to pale red (C2) as the particle aggregation proceeds. Heating of (C2), however, results in the return of the solution color to yellow (C1).

ized by their sharp DNA-melting transitions (full width at half-maximum (fwhm) = ~ 2 °C).

In a typical experiment, 1 OD of an oligonucleotide modified with three cyclic disulfide units (**1**, 5'-(DSP)₃-A₁₀-ATT-ATC-ACT-3'; **2**, 5'-(DSP)₃-A₁₀-AGT-GAT-AAT-3'; **DSP**, cyclic disulfide-containing phosphate derivative; see Figure 1A and Supporting Information) was added to 1 mL of Ag NP (31 nm in diameter, 1.2 nM) solution. The final oligonucleotide concentration is ~ 4.7 μ M, and the final Ag NP concentration is ~ 1 nM ($\epsilon_{410\text{ nm}} = 7.1 \times 10^8 \text{ cm}^{-1} \text{ M}^{-1}$).⁴⁰ This step was followed by the addition of 1% sodium dodecyl sulfate (SDS) aqueous solution (final concentration = 0.01% SDS) and 100 mM phosphate buffer (final concentration = 10 mM phosphate, pH 7.4). Over a period of 30 min, 2 M NaCl solution was added in a stepwise manner (final concentration = 0.15 M NaCl). The solution was incubated overnight at room temperature, followed by centrifugation to isolate the particles. The supernatant was removed, and the particles were redispersed in phosphate buffer (0.01% Tween 20, 10 mM phosphate, a desired concentration of NaCl, pH 7.4). This step was repeated three times to eliminate residual DNA. Equal concentrations of Ag NPs modified with sequence **1** or sequence **2** were combined and were allowed to hybridize at room temperature (Figure 1A).

To successfully immobilize oligonucleotides on the Ag NP surface, we first considered the interaction between the silver surface and the surface-binding groups of the oligonucleotides, which are affected by the number of binding groups. Recently, our group reported that multiple thiol groups increase the binding affinity of oligonucleotides for

the Au NP surface, which results in nanoparticle probes with higher stabilities.⁴¹ This strategy is based upon the fact that polydentate ligands often form more substantially stable metal-ligand complexes than monodentate ligands.⁴² Therefore, utilization of multiple anchoring groups on the oligonucleotides should lead to higher stability Ag NP-oligonucleotide conjugates. In addition, our group also demonstrated that oligonucleotides containing a cyclic disulfide-anchoring group bind readily to Au NPs with higher affinity than monothiol or acyclic disulfide groups.⁴³ Therefore, we designed an oligonucleotide sequence containing three cyclic disulfide moieties as anchoring groups (Figure 1A).

To study the properties of DNA-Ag NPs, two batches of silver nanoparticles were functionalized with complementary oligonucleotide sequences (sequence **1** and **2**, respectively), Figure 1A. Unmodified silver nanoparticles exhibit a surface plasmon resonance at 410 nm (Figure 1B), and therefore they exhibit an intense yellow color (Figure 1C-1). Interestingly, when Ag NPs are modified with either sequence **1** or **2**, respectively, they do not show any noticeable changes in their UV-vis spectrum, indicating that the particles are stable and do not aggregate. This has been confirmed by transmission electron microscopy (TEM) analysis of the modified particles (see Supporting Information). However, when DNA-Ag NPs, modified with complementary sequences **1** and **2**, respectively, are combined, the plasmon resonance dampens and red shifts from 410 to 560 nm (Figure 1B). This dampening and red shifting is a result of particle assembly due to hybridization, which can be observed with the naked eye in the form of a color change from bright

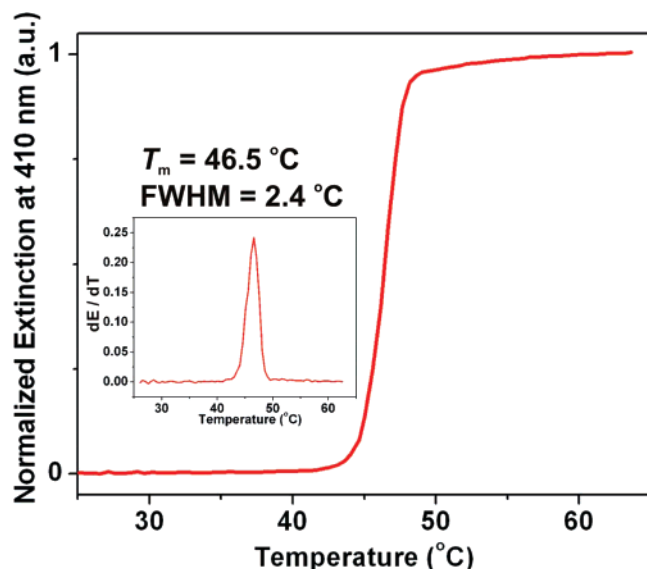


Figure 2. The melting transition for the DNA–Ag NP aggregates as monitored by the extinction of the Ag nanoparticles at 410 nm as a function of temperature ($T_m = 46.5$ °C). The concentration of nanoparticles is 1 nM (total). Note that the melting temperature is 46.5 °C, and the melting transition is extremely sharp (fwhm = 2.4 °C), which is comparable to that of DNA–Au NP aggregates.

yellow to pale red (Figure 1C). Because the process is due to DNA hybridization, it is reversible, and upon heating the color of the solution returns to an intense yellow, which is a diagnostic indicator of dehybridization in this system. (Figure 1C-1).

The reversible nature of the DNA–Ag NP hybridization process was further characterized by monitoring the melting process at 410 nm as a function of temperature (Figure 2). Importantly, the DNA-linked Ag NPs exhibit a sharp melting transition similar to that characteristic of the analogous DNA-linked Au NP aggregates,⁴ indicating that DNA-linked Ag NPs also exhibit highly cooperative binding properties. The melting temperature (T_m) of the DNA-linked Ag NPs, 46.5 °C, was obtained by taking the maximum of the first derivative of the melting profile. The fwhm of the first derivative (Figure 2, inset) is ~ 2.4 °C, which is comparable to the typical sharp melting transition of DNA-linked Au NPs (fwhm = ~ 2.2 °C).²⁴ Significantly, this melting transition was found to be highly reproducible, as demonstrated by repeated hybridization/melting experiments, which were performed with the same sample of the DNA–Ag NPs over a period of one week (see Supporting Information). This reproducibility is strong evidence that the modification of the Ag NP surface with oligonucleotides through a triple cyclic disulfide anchor is strong enough to stabilize the DNA–Ag NP probes against heat, aging, and degradation in aqueous media.

To determine the effect of the salt concentration on the melting properties of DNA–Ag NP aggregates, we monitored the melting transitions of DNA–Ag NP aggregates as a function of NaCl concentration. As expected, the melting transitions occur at higher temperatures as the salt concentration increases due to enhanced screening, which decreases the repulsion between the negatively charged oligonucleo-

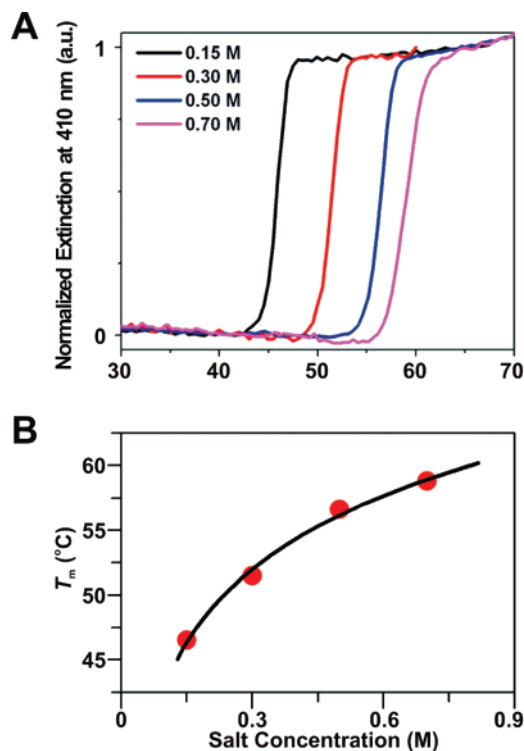


Figure 3. (A) Melting transitions for DNA–Ag NP aggregates (31 nm in diameter) at various salt concentrations: 0.15, 0.30, 0.50, and 0.70 M. The concentration of Ag NPs is 1 nM (total). (B) A plot of T_m as a function of salt concentration.

tides, as previously reported with DNA–Au NPs (Figure 3A).⁴ The T_m spans the range from 46.5 to 58.8 °C, as the salt concentration is increased from 0.15 to 0.70 M (Figure 3B). Note that the functionalized Ag NPs are stable at high-salt concentrations (up to 1.0 M NaCl). Importantly, all of the melting transitions are extremely sharp over the entire salt concentration range studied (fwhm $\leq \sim 2.5$ °C). This observation demonstrates that one can control the DNA–Ag NP hybridization and dehybridization process by adjusting salt concentrations similar to the control afforded by DNA–Au NPs.

In conclusion, we have developed a method for synthesizing stable DNA-functionalized silver nanoparticles that exhibit distant-dependent optical properties and highly cooperative binding properties, as demonstrated by sharp melting transitions. This method takes advantage of the strong affinity of multiple cyclic disulfide-anchoring moieties for the silver nanoparticle surface. This work is important as it (1) allows one to use Ag NPs in programmable material syntheses and as biodiagnostic probes with highly advanced functionalities, (2) demonstrates the use of cyclic disulfide moieties as anchoring groups on a silver nanoparticle surface, and (3) in principle, should be applicable to the functionalization of anisotropic silver nanomaterials with DNA.^{44–47}

Acknowledgment. C.A.M. acknowledges AFOSR, NSEC/NSF, and NCI-CCNE for support of this research. C.A.M. is also grateful for a NIH Director's Pioneer Award.

Supporting Information Available: Materials, experimental details for the oligonucleotide synthesis, TEM

Analysis, and repeated melting experiments of DNA–Ag NP aggregates. This material is available free of charge via the Internet at <http://pubs.acs.org>.

References

- (1) Mirkin, C. A.; Letsinger, R. L.; Mucic, R. C.; Storhoff, J. J. *Nature* **1996**, *382*, 607–609.
- (2) Alivisatos, A. P.; Johnsson, K. P.; Peng, X.; Wilson, T. E.; Loweth, C. J.; Bruchez, M. P.; Schultz, P. G. *Nature* **1996**, *382*, 609–611.
- (3) Storhoff, J. J.; Lazarides, A. A.; Mucic, R. C.; Mirkin, C. A.; Letsinger, R. L.; Schatz, G. C. *J. Am. Chem. Soc.* **2000**, *122*, 4640–4650.
- (4) Jin, R.; Wu, G.; Li, Z.; Mirkin, C. A.; Schatz, G. C. *J. Am. Chem. Soc.* **2003**, *125*, 1643–1654.
- (5) Lytton-Jean, A. K. R.; Mirkin, C. A. *J. Am. Chem. Soc.* **2005**, *127*, 12754–12755.
- (6) Lee, J.-S.; Stoeva, S. I.; Mirkin, C. A. *J. Am. Chem. Soc.* **2006**, *128*, 8899–8903.
- (7) Niemeyer, C. M.; Simon, U. *Eur. J. Inorg. Chem.* **2005**, 3641–3655.
- (8) Rosi, N. L.; Mirkin, C. A. *Chem. Rev.* **2005**, *105*, 1547–1562.
- (9) Nam, J.-M.; Thaxton, C. S.; Mirkin, C. A. *Science* **2003**, *301*, 1884–1886.
- (10) Stoeva, S. I.; Lee, J.-S.; Thaxton, C. S.; Mirkin, C. A. *Angew. Chem., Int. Ed.* **2006**, *45*, 3303–3306.
- (11) Liu, J.; Lu, Y. *Angew. Chem., Int. Ed.* **2006**, *45*, 90–94.
- (12) Lee, J.-S.; Han, M. S.; Mirkin, C. A. *Angew. Chem., Int. Ed.* **2007**, *46*, 4093–4096.
- (13) Cerruti, M. G.; Sauthier, M.; Leonard, D.; Liu, D.; Duscher, G.; Feldheim, D. L.; Franzen, S. *Anal. Chem.* **2006**, *78*, 3282–3288.
- (14) He, L.; Musick, M. D.; Nicewarner, S. R.; Salinas, F. G.; Benkovic, S. J.; Natan, M. J.; Keating, C. D. *J. Am. Chem. Soc.* **2000**, *122*, 9071–9077.
- (15) Pavlov, V.; Xiao, Y.; Shlyahovsky, B.; Willner, I. *J. Am. Chem. Soc.* **2004**, *126*, 11768–11769.
- (16) Niemeyer, C. M. *Angew. Chem., Int. Ed.* **2001**, *40*, 4128–4158.
- (17) Huang, C.-C.; Huang, Y.-F.; Cao, Z.; Tan, W.; Chang, H.-T. *Anal. Chem.* **2005**, *77*, 5735–5741.
- (18) Su, M.; Li, S.; Dravid, V. P. *Appl. Phys. Lett.* **2003**, *82*, 3562–3564.
- (19) Han, M. S.; Lytton-Jean, A. K. R.; Oh, B.-K.; Heo, J.; Mirkin, C. A. *Angew. Chem., Int. Ed.* **2006**, *45*, 1807–1810.
- (20) Maxwell, D. J.; Taylor, J. R.; Nie, S. J. *J. Am. Chem. Soc.* **2002**, *124*, 9606–9612.
- (21) Sato, K.; Hosokawa, K.; Maeda, M. *J. Am. Chem. Soc.* **2003**, *125*, 8102–8103.
- (22) Li, H.; Rothberg, L. J. *J. Am. Chem. Soc.* **2004**, *126*, 10958–10961.
- (23) Rosi, N. L.; Giljohann, D. A.; Thaxton, C. S.; Lytton-Jean, A. K. R.; Han, M. S.; Mirkin, C. A. *Science* **2006**, *312*, 1027–1030.
- (24) Storhoff, J. J.; Elghanian, R.; Mucic, R. C.; Mirkin, C. A.; Letsinger, R. L. *J. Am. Chem. Soc.* **1998**, *120*, 1959–1964.
- (25) Han, M. S.; Lytton-Jean, A. K. R.; Mirkin, C. A. *J. Am. Chem. Soc.* **2006**, *128*, 4954–4955.
- (26) Nam, J.-M.; Stoeva, S. I.; Mirkin, C. A. *J. Am. Chem. Soc.* **2004**, *126*, 5932–5933.
- (27) Cao, Y.; Jin, R.; Mirkin, C. A. *J. Am. Chem. Soc.* **2001**, *123*, 7961–7962.
- (28) Braun, G.; Lee, S. J.; Dante, M.; Nguyen, T.-Q.; Moskovits, M.; Reich, N. *J. Am. Chem. Soc.* **2007**, *129*, 6378–6389.
- (29) Mulvaney, P. *Langmuir* **1996**, *12*, 788–800.
- (30) Link, S.; Wang, Z. L.; El-Sayed, M. A. *J. Phys. Chem. B* **1999**, *103*, 3529–3533.
- (31) Jiang, Z.-J.; Liu, C.-Y.; Sun, L.-W. *J. Phys. Chem. B* **2005**, *109*, 1730–1735.
- (32) Hurst, S. J.; Lytton-Jean, A. K. R.; Mirkin, C. A. *Anal. Chem.* **2006**, *78*, 8313–8318.
- (33) Demers, L. M.; Mirkin, C. A.; Mucic, R. C.; Reynolds, R. A.; Letsinger, R. L.; Elghanian, R.; Viswanadham, G. *Anal. Chem.* **2000**, *72*, 5535–5541.
- (34) Tokareva, I.; Hutter, E. *J. Am. Chem. Soc.* **2004**, *126*, 15784–15789.
- (35) Vidal, B. C.; Deivaraj, T. C.; Yang, J.; Too, H.-P.; Chow, G.-M.; Gan, L. M.; Lee, J. Y. *New. J. Chem.* **2005**, *29*, 812–816.
- (36) Yin, Y.; Li, Z.-Y.; Zhong, Z.; Gates, B.; Xia, Y.; Venkateswaran, S. *J. Mater. Chem.* **2002**, *12*, 522–527.
- (37) Liu, S.; Zhang, Z.; Han, M. *Anal. Chem.* **2005**, *77*, 2595–2600.
- (38) Quaroni, L.; Chumanov, G. *J. Am. Chem. Soc.* **1999**, *121*, 10642–10643.
- (39) Chen, Y.; Aveyard, J.; Wilson, R. *Chem. Commun.* **2004**, 2804–2805.
- (40) The molar extinction coefficient is calculated from the measured UV–vis extinction of a colloid and a particle concentration known from the manufacturer.
- (41) Li, Z.; Jin, R.; Mirkin, C. A.; Letsinger, R. L. *Nucleic Acids Res.* **2002**, *30*, 1558–1562.
- (42) Cotton, F. A.; Wilkinson, G.; Murillo, C. A.; Bochmann, M. *Advanced Inorganic Chemistry*, 6th ed.; John Wiley & Sons: New York, 1999; pp 27–29.
- (43) Letsinger, R. L.; Elghanian, R.; Viswanadham, G.; Mirkin, C. A. *Bioconjugate Chem.* **2000**, *11*, 289–291.
- (44) Jin, R.; Cao, Y.; Mirkin, C. A.; Kelly, K. L.; Schatz, G. C.; Zheng, J. G. *Science* **2001**, *294*, 1901–1903.
- (45) Hao, E.; Kelly, K. L.; Hupp, J. T.; Schatz, G. C. *J. Am. Chem. Soc.* **2002**, *124*, 15182–15183.
- (46) Wiley, B.; Herricks, T.; Sun, Y.; Xia, Y. *Nano Lett.* **2004**, *4*, 1733–1739.
- (47) Jana, N. R.; Gearheart, L.; Murphy, C. J. *Chem. Commun.* **2001**, 617–618.

NL071108G